



HHS Public Access

Author manuscript

Biochim Biophys Acta Mol Cell Biol Lipids. Author manuscript; available in PMC 2023 January 01.

Published in final edited form as:

Biochim Biophys Acta Mol Cell Biol Lipids. 2022 January ; 1867(1): 159064. doi:10.1016/j.bbaliip.2021.159064.

Heparin binding triggers human VLDL remodeling by circulating lipoprotein lipase: Relevance to VLDL functionality in health and disease

Shobini Jayaraman^{1,*}, Antonio Pérez^{2,3}, Inka Miñambres², Jose Luis Sánchez-Quesada^{3,4}, Olga Gursky¹

¹Department of Physiology & Biophysics, Boston University School of Medicine, Boston, MA 02118, USA.

²Endocrinology Department of the Hospital de la Santa Creu i Sant Pau, Barcelona, Spain.

³CIBER of Diabetes and Metabolic Diseases (CIBERDEM), Spain.

⁴Cardiovascular Biochemistry Group, Research Institute of the Hospital de Sant Pau, CIBERDEM, Barcelona, Spain.

Abstract

Hydrolysis of VLDL triacylglycerol (TG) by lipoprotein lipase (LpL) is a major step in energy metabolism and VLDL-to-LDL maturation. Most functional LpL is anchored to the vascular endothelium, yet a small amount circulates on TG-rich lipoproteins. As circulating LpL has low catalytic activity, its role in VLDL remodeling is unclear. We use pre-heparin plasma and heparin-sepharose affinity chromatography to isolate VLDL fractions from normolipidemic, hypertriglyceridemic, or type-2 diabetic subjects. LpL is detected only in the heparin-bound fraction. Transient binding to heparin activates this VLDL-associated LpL, which hydrolyses TG, leading to gradual VLDL remodeling into IDL/LDL and HDL-size particles. The products and the timeframe of this remodeling closely resemble VLDL-to-LDL maturation *in vivo*. Importantly, the VLDL fraction that does not bind heparin is not remodeled. This relatively inert LpL-free VLDL is rich in TG and apoC-III, poor in apoE and apoC-II, shows impaired functionality as a substrate for the exogenous LpL or CETP, and likely has prolonged residence time in blood, which is expected to promote atherogenesis. This non-bound VLDL fraction increases in hypertriglyceridemia and in type-2 diabetes but decreases upon diabetes treatment that restores the glycemic control. In stark contrast, heparin binding by LDL increases in type-2 diabetes triggering

*Corresponding author. shobini@bu.edu.

Authorship contribution statement

Shobini Jayaraman: Conceptualization, Investigation, Formal analysis, Writing - original draft & editing. Antonio Pérez: Resources. Inka Miñambres: Resources. Jose Luis Sánchez-Quesada: Resources, Writing – review & editing, Funding acquisition. Olga Gursky: Writing - original draft & editing, Formal analysis, Funding acquisition.

Declaration of competing interest

The authors declare that they have no known competing financial interests or personal relationships that could have appeared to influence the work reported in this paper.

Publisher's Disclaimer: This is a PDF file of an unedited manuscript that has been accepted for publication. As a service to our customers we are providing this early version of the manuscript. The manuscript will undergo copyediting, typesetting, and review of the resulting proof before it is published in its final form. Please note that during the production process errors may be discovered which could affect the content, and all legal disclaimers that apply to the journal pertain.

pro-atherogenic LDL modifications. Therefore, the effects of heparin binding are associated negatively with atherogenesis for VLDL but positively for LDL. Collectively, the results reveal that binding to glycosaminoglycans initiates VLDL remodeling by circulating LpL, and suggest heparin binding as a marker of VLDL functionality and a readout for treatment of metabolic disorders.

Keywords

VLDL remodeling and maturation; lipoprotein lipase activity; lipoprotein binding to glycosaminoglycans; hypertriglyceridemia, type-2 diabetes and cardiovascular disease; heparin-sepharose affinity chromatography

1. INTRODUCTION

VLDL is the major plasma carrier of TG and the direct metabolic precursor of IDL and LDL. The crucial step in VLDL metabolism and maturation to LDL is TG hydrolysis into glycerol and non-esterified fatty acids (NEFA), which are utilized by cells for energy expenditure (e.g. in cardiac and skeletal muscle) or for storage (in adipose tissue) [1]. Lipolysis of VLDL TG is mediated primarily by the lipoprotein lipase (LpL), followed by the hepatic lipase [1–3]. As the TGs in the particle core are hydrolyzed, VLDLs are remodeled into smaller remnant particles, IDL or light LDL. In this process, termed the lipolytic cascade, the excess surface moieties are released from VLDL in the form of apoE-containing HDL and lipid-poor proteins, mainly apoCs, which associate with HDL [3–5]. IDL are then cleared from circulation via the endocytosis (mediated by the LDL receptor-related protein, LDL receptor, or apoE receptor) or are ultimately converted into mature LDL. When this process is impaired, e.g. due to inefficient hydrolysis of plasma TG, the residence time of VLDL in plasma increases, leading to progressive post-translational VLDL modifications such as oxidation, hydrolysis and, ultimately, formation of highly pro-atherogenic TG-rich small dense LDL [6–9] and electronegative LDL [10]. Therefore, efficient hydrolysis of VLDL TG followed by lipoprotein clearance is important for cardiovascular health. Conversely, in metabolic disorders such as hypertriglyceridemia, metabolic syndrome and type-2 diabetes, TG metabolism is impaired and plasma levels of VLDL TG are elevated, providing a causative risk factor for cardiovascular disease [1, 3, 8, 9]. Therefore, elevated TG levels in VLDL and their remnants are a therapeutic target in cardiovascular disease [11, 12].

Hydrolysis of TG-rich lipoproteins by LpL is essential for nutrient delivery to cells and is tightly regulated in response to changes in the nutrition status and cellular demands for energy [2]. Lipolytic activity of LpL is regulated by multiple factors including LpL self-association; binding to proteoglycans (PG) in vascular endothelium; LpL interactions with various activators (e.g. apoC-II) or inhibitors (apoC-III and apoC-I); substrate availability, etc. (reviewed in [2, 3, 13, 14]). High-resolution structural studies of LpL in various forms have provided snapshots of alternative lipase conformations with varying activity [15–17]. This helps to understand how LpL activity is regulated by the access to the catalytic site, folding of the catalytic domain, relative packing of the catalytic and lipid-binding

domains, protein self-association, and interactions with cofactors [13, 14, 17]. For example, polyanionic cofactors such as GPIHBP1 peptide or heparin sulfate (HS) moieties of PGs are inferred to increase LpL activity by binding to the large basic surface spanning both lipase domains [15, 16]. Still, molecular details of LpL binding to HS and how it stabilizes the catalytically active LpL conformation(s) are unknown.

Most plasma TGs are hydrolyzed by LpL anchored to the vascular endothelium via the GPIHBP1 peptide; the peptide transports LpL from the interstitial space wherein LpL is membrane-anchored via HSPGs ([15, 16] and references therein). However, a small amount of LpL circulates bound to TG-rich lipoproteins such as VLDL, chylomicrons, and their remnants ([18–20] and references therein). The catalytic activity of this circulating LpL and its role in lipoprotein remodeling is unclear. Some studies reported that circulating LpL is catalytically inactive and functions primarily to bridge the lipoproteins to their receptors or to HSPGs in the vascular endothelium ([18, 21] and references therein) and also to stimulate TG transfer to HDL and LDL via the cholesterol ester transfer protein (CETP) [22]. Others reported that VLDL-bound LpL has substantial lipolytic activity that correlates strongly with VLDL remodeling in plasma [19, 20]. The current study addresses the catalytic activity of circulating LpL and its role in VLDL remodeling by exploring VLDL–heparin interactions.

Both VLDL and LDL bind HSPGs and their highly sulfated mimetic, heparin; however, the molecular basis for these interactions and their biological ramifications are distinctly different. LDL binds HS and heparin mainly via the basic residues in apoB [23, 24]. The binding enhances LDL retention and remodeling in the arterial intima, which is proposed to initiate atherosclerosis [24–26]. In contrast, VLDL binds HS and heparin mainly via the basic sites in apoE [23] and other minor proteins such as LpL [28, 29]. VLDL binding to HSPGs in vascular endothelium may have multiple effects. First, the binding may enhance the sub-endothelial retention of small VLDL, although apoE and LpL may mitigate this pro-atherogenic effect [29]. Second, the binding co-localizes VLDL with endothelial LpL and with VLDL receptors, thereby augmenting VLDL lipolysis and receptor-mediated endocytosis. Although the latter mechanism is non-atherogenic in the arterial endothelium, it can be pathogenic in other contexts [30] including VLDL co-localization and whole-particle uptake via the scavenger receptors on arterial macrophages or cancer cells. In fact, this mechanism was proposed to contribute to the lipid dependency of breast cancer cells wherein VLDL binding to cell surface PGs helps co-localize VLDL with CD36 receptor, thereby augmenting receptor-mediated VLDL endocytosis [31].

In metabolic disorders such as type-2 diabetes, LDL binding to HSPGs and heparin increases due to changes in both PGs and lipoproteins, such as lipoprotein glycation, oxidation and hydrolysis ([26] and references therein). Moreover, HSPG binding causes irreversible structural alterations in LDL, promotes LDL fusion, and makes it more susceptible to oxidation and hydrolysis; in diabetes, these deleterious LDL alterations are enhanced, contributing to a causal link between diabetes and atherosclerosis [26]. In the current study we explore how binding to heparin influences the structural and biochemical properties of VLDL isolated from healthy subjects and from patients with metabolic disorders including hypertriglyceridemia and type-2 diabetes. The results reveal striking differences in the effects of heparin binding on LDL and VLDL.

2. MATERIALS AND METHODS

2.1 Proteins

Secretory group-II phospholipase A₂ (PLA₂) from honeybee venom (#P9279), sphingomyelinase (SMase) from *Bacillus cereus* (#S9396), lipoprotein lipase (LpL) from porcine pancreas (#L3126) or milk (#L2254), cholesterol esterase (CEase) from *Pseudomonas fluorescens* (#C9281), trypsin (#T1426), the essentially fatty acid-free human serum albumin (#A1887), and recombinant human CETP (#SRP6177) were from Sigma. The primary antibody for apoB was rabbit polyclonal anti-apoB (#ab27626, Abcam) and the secondary was goat-anti-rabbit horseradish peroxidase-conjugated antibody (#B-1215, Boston Bioproducts); the primary antibody for LpL was from Millipore Sigma (#MABS1350); the primary antibody for lipoprotein-associated PLA₂ was from Biorbyt (#orb243886). All chemicals were of highest purity analytical grade.

2.2 Lipoprotein isolation

Single-donor human VLDL were isolated from the EDTA-treated plasma of ten anonymous healthy volunteers after an overnight 12 h fast. No heparin injection was administered prior to blood donation. Blood was collected in EDTA-containing Vacutainer tubes. The plasma was purchased from a blood bank Research Blood Components LLC (Boston, USA) in compliance with the Institutional Review Board. Chylomicrons were removed by ultracentrifugation at 30,000 rpm for 45 min at 11 °C. VLDL (density range 0.94–1.006 g/mL), LDL (1.019–1.063 g/ml) and HDL (1.063–1.21 g/ml) were isolated by sequential preparative KBr density gradient ultracentrifugation as described previously [32] [Jayaraman et al., 2019]. Immediately after isolation, lipoproteins were extensively dialyzed at 4 °C against buffer A (10 mM sodium phosphate, 150 mM NaCl, pH 7.4). Lipoprotein stock solution containing 0.5 mg/ml total protein in 20% sucrose was aliquoted in 0.5 ml and frozen at –80 °C. Each aliquot was thawed, dialyzed against buffer A, and used within two weeks, during which no protein degradation was detected by SDS PAGE and no changes in the lipoprotein electrophoretic mobility were seen on the agarose gel.

To test if VLDL freezing and storage in 20% sucrose altered VLDL properties, control experiments were performed using fresh VLDL (no sucrose, no freezing) and the same sample after 6–12 month storage in 20% sucrose and one freeze-thaw cycle. Representative results in supplemental Figure S1 show minimal or no significant changes in the properties of VLDL determined in the current study, including particle size distribution, heparin binding affinity, or LpL-mediated TG-hydrolysis. Therefore, VLDL storage in 20% sucrose did not affect the results of the current study.

To compare human VLDL from healthy and diabetic subjects, five different batches of pooled plasma were used. Each batch contained plasma from 20 healthy normolipemic and normoglycemic (NI) volunteers and from 20 patients who have been diagnosed with type-2 diabetes and presented a poorly controlled (Pc) glycemic index (hemoglobin A1c, HbA1c 7.5%). Depending on the clinical presentation, these patients were subjected to hypoglycemic treatment including diet, exercise, metformin and insulin. The treatment improved the patients' glycemic control (HbA1c<7% and/or a decrease by at least 1.5%

below the baseline value), which we termed good glycemic control (Gc); for additional details see [32]. Plasma was obtained at the Hospital de Sant Pau (Barcelona, Spain) with written informed consent by the patients and upon approval by the institutional ethics committee. The plasma was pooled for NI, Pc and Gc patients and VLDL were isolated by sequential density ultracentrifugation.

2.3 Electron microscopy

VLDL were visualized by transmission electron microscopy with a CM12 microscope (Philips Electron Optics, the Netherlands). Briefly, a 4 μ L VLDL aliquot (0.1 mg/ml total protein) in buffer A was incubated for 1 min on a carbon, formvar-coated 300 mesh grid (#FCF300-CU-TB, Electron Microscopy Sciences). After blotting excess fluid, the grid was washed thrice with buffer A, negatively stained with 1% uranyl acetate, blotted, and air-dried. Images were recorded with a 50,000x magnification on a 2Kx2K CCD camera (24 microns/pixel) and processed in Adobe Photoshop.

2.4 Protein and lipid quantification

Total protein concentration was determined using a modified Lowry assay with bovine serum albumin as a standard. ELISA was used to quantify the following proteins: apoB (Abcam, cat. #ab108807, lot #GR3266113), apoE (Abcam, cat. #ab233623, lot #GR3365265), apoC-III (Abcam, cat. #ab154131, lot #GR3361085), apoC-II (Abcam, cat. #ab168549, lot #GR3364209), apoC-I (Santa Cruz Biotechnology, cat. #sc-101263), and LpL (Biorbyt, cat. #orb562265); ultrapure synthetic human apoC-I (21st Century Biochemicals) was used to generate the standard curve for apoC-I (6 kDa). Cholesterol, TG, and phospholipids were quantified using enzymatic assays as previously described [32]. NEFA were measured using an enzymatic colorimetric assay (Enzymchrom™ free fatty acid kit, #EFA-100, Fisher Scientific). All concentrations were measured in technical triplicates.

2.5 Liquid chromatography, gel electrophoresis, and immunoblotting

Liquid chromatography was performed using an ÄKTA UPC 10 FPLC system (GE Healthcare). For size-exclusion chromatography (SEC), a Superose 6 10/300 GL column was used. VLDL was eluted by buffer A at a flow rate of 0.5 ml/min. The void volume (7.7 ml) was determined using freshly prepared blue dextran (Sigma, #D4772) run under the same conditions as VLDL. For heparin affinity chromatography, HiTrap-HP column (GE Life Sciences, #17040601) was used. The column was equilibrated with 5 volumes of buffer A. VLDL solution (0.5–1.0 ml of 0.5 mg/ml total protein concentration) was filtered with a 0.2 micron filter, loaded onto the column, and incubated for 10 min. The flow-through fraction was eluted with 3 column volumes of buffer A, and the bound fraction was eluted with 3 volumes of buffer B (10 mM sodium phosphate buffer, 1.0 M NaCl, pH 7.4) using a linear gradient from 0 to 100% of buffer B. These fractions were collected, immediately dialyzed against buffer A, stored at 4 °C, and used for further studies that were completed within 30 hours. To mimic VLDL fraction that eluted from the heparin column at 0.4–0.5 NaCl, VLDL were exposed to 0.5 M NaCl for 20 min followed by dialysis against buffer A. No VLDL modifications were detected upon this treatment.

For dot blot analysis, 5 μ l of VLDL sample (1 mg/ml protein in buffer A) was spotted on a nitrocellulose membrane (Fisher, #09–301-109) and dried. To ensure the VLDL load, the membrane was sliced into two parts; one part was probed for apoB and the other for LpL. The membranes were rinsed with distilled water and blocked in 5% w/v nonfat dry milk in Tween-20 (Boston Bioproducts, #IBB-181) for 1 h at 24 °C. Next, the membranes were incubated at 4 °C overnight with the primary antibodies (anti-LpL or anti-apoB) which were diluted 1:1000 in 5% nonfat dry milk in TBS with TWEEN-20. The blots were washed thrice in TBS with TWEEN-20 and then incubated at 24 °C for 1 h with secondary antibodies, which were diluted 1:5000 in TBS with TWEEN-20. The membranes were washed thrice with TWEEN-20. The signal was developed with Thermo Scientific™ SuperSignal™ West Femto Chemiluminescent Substrate (Fisher, #PI34095). Images were collected with KwikQuant imager. Exposures from 1 s to 4 min were used; the 30 s exposure was shown in the figures.

2.6 Preparation and characterization of modified VLDL

For spontaneous lipolysis, freshly isolated VLDL (0.3 μ mol TG) was incubated at 37 °C in 0.5 mL of 10 mM PBS, pH 7.4, and the time course of the total lipolysis was monitored by quantifying NEFA. Blanks were obtained in similar experiments performed in the presence of 2 μ mol/ml paraoxon (E600, Sigma, St. Louis, MO) to block enzymatic lipolysis. Blanks were subtracted from the data; the difference represented NEFA released upon lipolysis of TG by LpL. To ensure that endogenous LpL was solely responsible for the spontaneous lipolysis, we tested VLDL for the presence of lipoprotein-associated PLA₂; both ELISA and SDS PAGE of VLDL probed with antibodies for this PLA₂ showed negative results.

For limited lipolysis of specific lipids by exogenous lipases, VLDL (0.5 mg/ml apoB) was incubated for 3 h at 37 °C in buffer C (150 mM NaCl, 2 mM CaCl₂, 2 mM MgCl₂, 20 mM Tris HCl, pH 7.0) containing 2.5 mg/ml albumin and one of the following lipases: 10 μ g/ml sPLA₂, 40 μ g/ml SMase, 25 U/ml LpL, or 50 mU/ml CEase. The lipolysis was stopped by adding EDTA to a final concentration of 10 mM. VLDL was re-isolated by SEC and used for heparin affinity chromatography on the same day. The degree of PLA₂- and LpL-induced lipolysis was determined by quantifying NEFA. The degree of the SMase-induced lipolysis was determined by quantifying phosphocholine using an Amplex Red sphingomyelinase assay kit (Thermo Fisher Scientific, #A12220). The degree of CEase-induced lipolysis was monitored by measuring the increase in free cholesterol using an EnzyChrom cholesterol assay kit (Fisher Scientific, #ECCH-100). Lipids hydrolyzed in these experiments comprised 20–25% of their initial levels in intact VLDL. Throughout this study we used porcine LpL from pancreas or from milk (as a control); both lipases yielded very similar results; the results using pancreatic LpL are presented.

For limited proteolysis, VLDL (0.5 mg/ml protein) was incubated with trypsin (200:1 substrate:enzyme wt:wt) for 3 h at 37 °C. The reaction was stopped using 1 mM phenylmethylsulfonyl fluoride (Sigma Aldrich, #93482).

For oxidation, the baseline levels of lipid oxidation were determined by measuring absorbance at 234 nm for conjugated dienes in freshly isolated VLDL (0.1 mg/ml total protein in buffer A) at 22 °C. The data are shown as an average of three independent

measurement \pm STD. Oxidized VLDL was obtained by incubating total VLDL (0.1 mg/ml total protein) with 10 μ M CuSO₄ at 37 °C for 24 h. The reaction was stopped by adding 2 mM EDTA and cooling the sample on ice, followed by extensive dialysis against buffer A before use.

2.7 TG transfer efficiency

VLDL were used as TG donors, HDL as TG acceptors, CETP as a vehicle for TG transfer, and albumin to remove the reaction products. First, VLDL and HDL were dialyzed against 50 mmol Tris, 0.01 % NaN₃ at pH 8.5. Next, VLDL (1mg/ml of total protein), HDL (1mg/ml of total protein), CETP (100 μ g/ml) and albumin (1mg/ml) were incubated for 2 h at 37 °C with mild shaking. VLDL and HDL were isolated by SEC from the incubation mixture and the TG levels were quantified.

2.8 Reproducibility

All experiments were repeated three to six times to ensure reproducibility. Studies of normolipidemic single-donor VLDL from group 2 were performed in technical triplicates using four different batches; studies of VLDL from groups 1 and 3 were performed in technical triplicates using three different batches. Studies of pooled lipoproteins from plasma of normolipidemic and diabetic patients were performed in technical triplicates using five different VLDL batches. All batches showed similar trends; the data for representative batches are shown. Statistical analysis was performed using ANOVA t-test. Moderate (p 0.1, **) and significant (p 0.05, ***) statistical differences are indicated in the data.

3. RESULTS

3.1 Human VLDLs show decreased heparin binding upon increased levels of plasma TG

Single-donor VLDL from healthy donors were grouped according to the plasma TG levels of these donors: TG < 100 mg/dl (group 1, N=3), 100 < TG < 200 mg/dl (group 2, N=4), and TG > 200 mg/dl (group 3, N=3). As expected, lipid assays showed that the TG levels in VLDL increased in order group 1 < group 2 < group 3, while the levels of cholesterol, particularly esterified cholesterol, decreased (Table 1). SEC showed two major particle size populations in VLDL from groups 1–3 (Figure 1A). The first peak at the void volume represented larger particles, termed VLDL₁ (peak I, 7.7 ml). An additional peak II centered circa 11 ml represented smaller particles, termed VLDL₂; in comparison, LDL migrated at 13 ml. VLDL subclasses were further assessed by separating total VLDL from groups 1 – 3 into two density fractions, large buoyant VLDL₁ and small dense VLDL₂, followed by SEC analysis (Supplemental Figure S2). The results showed that the positions of SEC peaks I and II were very similar for VLDL from groups 1 to 3, but the relative amount of VLDL₂ (peak II) progressively increased with decreasing TG in order group 3 < group 2 < group 1 (Figures 1A and S2). This finding was supported by electron micrographs showing more heterogeneous particles with a larger population of smaller particles in group 1 compared to groups 2 and 3 (Figure 1B). Moreover, native PAGE showed that groups 1 and 2 VLDL migrated as smaller particles compared to group 3 (Figure 1C). In addition to peaks I and II, a minor population, which was consistent with the lipid-poor/free proteins, was detected by SEC (~21 ml) but not by the native PAGE (Figure 1A, C).

Next, protein composition of VLDL from groups 1–3 was probed by SDS PAGE and ELISA. SDS PAGE detected apoC-II in VLDL from groups 1 and 2, but not 3; group 3 VLDL also showed lower content of apoE (Figure 1D). Consistent with these findings, ELISA showed that the levels of apoC-II and apoE decreased while apoC-III increased with increasing TG, from group 1 to 3 (Table 1). These results are consistent with previous reports of decreased apoE and increased apoC-III in hypertriglyceridemic VLDL ([33] and references therein).

Heparin affinity chromatography of group 1 VLDL showed two comparable-size fractions: the flow-through non-bound fraction eluted in 0 M NaCl (0.5–2 ml) and the bound fraction eluted in 0.3–0.5 M NaCl (8–12 ml) (Figure 1E). The amount of the bound fraction progressively decreased, and the peak shifted to lower salt from group 1 to group 3, with minimal binding detected in group 3 VLDL; hence, both the binding capacity and the binding affinity decreased upon increasing the TG levels (Figure 1E). Collectively, the results in Figure 1 and Table 1 showed that the fraction of heparin-bound VLDL increases with: i) decrease in TG and increase in cholesterol levels, ii) increase in apoE and apoC-II and decrease in apoC-III levels, iii) increased population of VLDL₂. These results are generally consistent with previous findings that, compared to non-bound VLDL, bound VLDL has lower TG content, higher apoE/apoC ratio, undergoes faster remodeling, and is higher in normolipidemic than in hyperlipidemic subjects ([34, 35] and references therein). In addition, our results clearly show that bound VLDL increases with increased apoC-II/apoC-III ratio (Table 1), which has important implications for LpL activity described below.

Non-bound and bound VLDL were isolated by heparin affinity chromatography and used within 24–30 hours, during which bound VLDL underwent rapid TG lipolysis and particle remodeling, as shown in Figures 2, 3 and Table 2 below. Limited sample availability permitted detailed studies of only group 2 VLDL. First, particle size distribution was probed by SEC 6 hours after VLDL isolation by heparin affinity. As in Figure 1A, native VLDL (prior to heparin affinity chromatography) in Figure 2A showed VLDL₁ (peak I) and VLDL₂ (peak II). These peaks were also observed in the non-bound fraction (wherein peak II shifted to larger particles, forming a shoulder of peak I), along with some lipid-poor proteins (peak IV), mainly apoC-I and apoC-III (as indicated by ELISA). In stark contrast, bound fraction contained a greatly reduced population of VLDL₁ (peak I), a well-resolved population of LDL-size particles (peak II'), and a large population of HDL-size particles (peaks III' and III, Figure 2A). These particles were also clearly seen in the bound fraction by electron microscopy and native PAGE (Figure 2B, C). Both SEC and native PAGE showed two distinct populations of HDL-size particles circa 8 nm and 10 nm (III' and III). These results indicate a dramatic remodeling of bound VLDL 6 hours after binding to the heparin column.

Next, the biochemical composition of native VLDL and its non-bound and bound fractions was quantified using lipid assays and ELISA. The non-bound fraction was enriched in TG while the bound fraction had very low levels of TG but high levels of NEFA as well as high cholesterol, especially cholesterol ester (Table 2). Furthermore, the non-bound fraction had high content of apoC-III but low apoC-II and low apoE, whereas the bound fraction had elevated apoE and apoC-II but low apoC-III (Table 2). ApoB levels were comparable in both fractions.

In summary, the non-bound and bound VLDL fractions have distinct biochemical composition and particle size distribution. Compared to the non-bound fraction, the bound fraction is TG-poor, NEFA-rich, cholesterol-rich, and comprises a heterogeneous population of VLDL, LDL and HDL-size particles. These results are consistent with “remnant-like” properties of bound VLDL including smaller particle size, reduced TG content, increased apoE content, and faster catabolism ([34, 35] and references therein). Since heparin binding is mediated primarily by apoE in VLDL and by apoB in LDL, high apoE content along with the presence of LDL-size particles in the bound fraction are expected to contribute to heparin binding. Another contributing factor to heparin binding, which explains a dramatic decrease in TG and an increase in NEFA in the bound fraction, is the presence of LpL in the bound VLDL (Table 2), described in part 3.3 below.

3.3 Heparin-induced VLDL remodeling results from activation of the endogenous LpL

Previously we showed that binding to heparin promotes pro-atherogenic modifications in LDL including lipoprotein hydrolysis and oxidation; NEFA generated in this process lead to particle remodeling and fusion [26]. To test whether binding to heparin triggers biochemical and morphological changes in VLDL, bound and non-bound fractions were freshly isolated by heparin affinity chromatography from group 2 VLDL and were immediately dialyzed against the low-salt buffer (buffer A); next, these fractions were incubated at 22 °C for 30 h, and NEFA content was quantified as a function of time. Native VLDL was used as a control. A hyperbolic increase in NEFA was observed in all VLDL samples during the first 5–6 hours of incubation, followed by saturation (Figure 3A). NEFA generation increased at 37 °C and decreased at 4°C (Figure 3B). The amplitude of this increase and the initial and final NEFA levels were much higher in the bound fraction *versus* either native or non-bound VLDL. Compared to native VLDL, non-bound VLDL showed slightly lower levels of NEFA, indicating that passing through the heparin column without binding did not promote the lipolysis. Therefore, enhanced lipolysis of the bound fraction must be triggered by VLDL binding to heparin. In summary, isolated VLDL undergoes spontaneous gradual lipolysis at 22 °C, which is greatly increased upon heparin binding.

Does this lipolysis induce VLDL remodeling into smaller particles? Bound fraction was incubated at 22 °C and aliquots taken at various times, from 0.5 h to 72 h, were probed by native PAGE (Figure 3C). Gradual remodeling of intact-size VLDL (band I) into smaller IDL/LDL-size (II') and HDL-size particles (III' and III) was observed. Figure 3C shows that HDL-size particles, which again comprised two populations circa 8 nm and 10 nm in size (III and III'), along with lipid-poor protein (IV) were first detected after 3 h, reached maximum at about 12 h, and gradually disappeared by ~32 h. The transient nature of these products could result, in part, from the gradual hydrolysis of phospholipids upon prolonged incubation with LpL. The exact timeline of this process varied from batch to batch, precluding more detailed analysis of the transient products. Notably, in bound VLDL, the time course of formation of HDL-size particles apparently followed the generation of NEFA (Figure 3A and 3C compared), suggesting a causal link between these events. Furthermore, in non-bound and in native VLDL, whose NEFA content was much lower compared to the bound fraction (Figure 3A, C), HDL-size particles were not detected during prolonged incubation at 22 °C (40 h to 72 h in Figure 3D, E). Taken together, these results

suggest that the formation of HDL-size particles follows VLDL lipolysis that is greatly enhanced upon heparin binding.

We conjectured that spontaneous VLDL lipolysis seen in Figures 3A, C is due, in part, to the endogenous LpL associated with VLDL. In fact, it has been previously reported that a small percentage of LpL circulates bound to TG-rich lipoproteins, including VLDL remnants, and can hydrolyze TG in these lipoproteins causing their remodeling *ex vivo* [21]. To test our conjecture, LpL levels in VLDL groups 1–3 were determined by ELISA. LpL content nearly doubled from group 1 to group 3 (Table 1).

Next, we tested the catalytic activity of endogenous VLDL-bound LpL. Freshly isolated VLDLs from groups 1 to 3 were incubated at 37 °C for up to 3 h without or with 2 $\mu\text{mol/ml}$ paraoxon, an inhibitor of lipases such as LpL. Since LpL is the major endogenous lipase on circulating VLDL, most lipolytic products such as NEFA must be generated upon TG hydrolysis by LpL. NEFA content was measured every 30 min, and the difference between the measurements without and with paraoxon, which represents NEFA produced upon enzymatic TG hydrolysis, was determined. Lipase activity was significantly higher in group 1 VLDL, followed by groups 2 and 3 (Figure 4A). Consequently, in groups 1–3, the degree of enzymatic lipolysis related directly to the population of IDL/LDL-size particles (Figure 1A), suggesting that these particles were the products of VLDL remodeling upon TG lipolysis.

These results indicate that the levels of VLDL-associated LpL increased with increasing TG levels (Table 1) while the LpL activity decreased (Figure 4A). This apparently paradoxical observation can be explained by the finding that the content of apoC-III, the LpL inhibitor, increased nearly 4-fold from group 1 to group 3, while the content of apoC-II, the LpL activator, decreased nearly two-fold, leading to greater LpL activity in group 1 (Table 1). Together, our results support the conjecture that progressive TG hydrolysis by the endogenous LpL is responsible for the spontaneous remodeling of VLDL into IDL/LDL-size and HDL particles. This remodeling is most advanced in group 1 VLDL (Figure 1A) where LpL activity is highest (Figure 4A, B) and the largest amount of TG has been hydrolyzed (Table 1), followed by groups 2 and 3.

Further support for the key role of the endogenous LpL in VLDL remodeling into smaller particles comes from the observation that such a remodeling is greatly augmented by binding to the heparin column (Figure 2). LpL is well known to be activated upon binding to heparin and HSPGs [13, 14, 28]. To probe this activation for circulating LpL, we tested if soluble heparin increases the activity of the VLDL-bound LpL. VLDL was incubated with or without heparin at 37 °C for 3 h, the lipolysis was stopped by paraoxon, and the NEFA content was measured. Heparin induced a significant increase in NEFA in all VLDL groups, particularly in group 1 where the pre-heparin LpL activity was highest, followed by groups 2 and 3 (Figure 4B). Taken together, the results in Figures 2 and 4 strongly support the lipolytic activity of the VLDL-bound LpL and indicate that this activity increases upon binding to heparin, either in solution or immobilized on the column.

Next, we tested whether the activation of the VLDL-bound LpL by heparin causes lipoprotein remodeling into smaller particles, such as those seen in bound VLDL from group 2 (Figure 2). Bound fraction was isolated from group 2 VLDL, whereupon 2 $\mu\text{mol/ml}$ paraoxon was immediately added to completely inhibit LpL. Bound VLDL with or without paraoxon, along with the non-bound fraction without paraoxon, were incubated at 37 °C for 3 h, followed by native PAGE analysis. HDL-size particles were observed only in the bound fraction without paraoxon, i. e. when LpL was active (Figure 4C). Importantly, LpL was detected by dot blot in native and in bound VLDL, but not in the non-bound fraction (Figure 4D). Together, these results clearly show that VLDL remodeling with the release of HDL-size particles occurs only in the presence of catalytically active LpL.

As an additional control, we tested how the activity of the exogenous LpL on VLDL is influenced by soluble heparin. Native VLDL was incubated with bovine LpL with or without heparin (1:1 wt/wt of total VLDL protein:heparin) for 3 h at 37 °C as described in Methods, and NEFA were measured as a function of time. Similar to the endogenous LpL, heparin significantly increased the catalytic activity of the exogenous LpL on VLDL (Figure S3).

Collectively, our results clearly show that binding to heparin, either in solution or immobilized on the Sepharose, increases the activity of the VLDL-associated LpL. This activity promotes VLDL remodeling into IDL/LDL-size particles followed by the release of the HDL-size particles and excess proteins. The extent of this remodeling increases with increasing the content of apoC-II, which activates LpL, and decreasing apoC-III, which inhibits LpL (Table 1). Furthermore, HDL-size particles are detected neither in non-bound VLDL, which lacks LpL (Figure 4A), nor in the bound fraction with paraoxon, which inhibits LpL (Figure 4D). These findings illustrate the complex regulation of the enzymatic LpL activity by multiple factors, including HSPG, proteins such as apoCs, and lipids [14].

3.4 TG lipolysis by LpL: time course and effects on heparin binding and VLDL remodeling

Next, we explored in detail the time course of TG hydrolysis by LpL and the ensuing VLDL remodeling. Group 2 VLDL was incubated with exogenous LpL at 37 °C for up to 24 h, and the TG lipolysis was monitored by measuring NEFA over time. The initial hyperbolic increase in NEFA leveled off after about 6 h (Figure 5A). VLDL at various stages of lipolysis were subjected to native PAGE and SEC (Figure 5B, C). An increased population of IDL/LDL-size particles was observed between 1 h and 3 h of incubation with LpL. This was followed by the formation of HDL-size particles circa 6 h (Figure 5B, C); at this stage, the NEFA levels approached saturation (Figure 5A). Heparin affinity profiles showed an increased population of bound VLDL during the first hour of lipolysis, with only minor changes at later times. Therefore, LpL lipolysis and NEFA generation first lead to increased heparin binding and to formation of IDL/LDL-size particles, followed by formation of HDL-size particles.

Moreover, comparison of the native PAGE and SEC data labeled “6 h” in Figure 5 B and C with similar data labeled “bound” in Figure 2A and C showed that changes in the particle size distribution upon VLDL remodeling by the exogenous LpL were strikingly

similar to those observed after VLDL binding to heparin. This similarity strongly supports our conclusion that that activation of the endogenous LpL upon heparin binding promotes VLDL remodeling into IDL/LDL and HDL-size particles.

Taken together, our results show that VLDL binding to heparin increases the LpL activity (Figure 3), while LpL activity increases VLDL binding to heparin (Figure 5). This suggests a synergy between hydrolysis of VLDL TG by LpL and VLDL binding to heparin. Furthermore, regardless of the origin of LpL (endogenous or exogenous), the action of LpL with or without activation by heparin (Figures 3, 5) leads to very similar VLDL remodeling into IDL/LDL and, ultimately, HDL-size particles.

3.5 Effects of lipolysis, proteolysis and oxidation on VLDL particle remodeling

How does VLDL remodeling by LpL compare to that of other lipases that act on plasma lipoproteins *in vivo*? To test how lipolysis of specific lipids affects the particle size distribution and heparin binding, group 2 VLDL was hydrolyzed by exogenous lipases for 3–6 h at 37 °C as described in Methods. To hydrolyze surface lipids, we used group-IIa secretory PLA₂ (for total phospholipids) and SMase (for sphingomyelin alone); to hydrolyze core lipids, we used CEase (for cholesterol esters) and LpL (for TG). The particle size distribution before and after 3 h of lipolysis was analyzed by SEC and native PAGE (Figure 6A, B). Phospholipid hydrolysis by either PLA₂ or SMase led to decreased levels of VLDL₂/IDL/LDL-size particles in group 2 VLDL. CE hydrolysis nearly eliminated these particles, suggesting that, like plasma LDL, these particles were CE-rich. In stark contrast, TG hydrolysis by LpL led to a large increase in the population of VLDL₂/IDL/LDL-size particles observed by SEC (Figure 6A). IDL/LDL and HDL-size particles became apparent on the native PAGE after 6 hours of lipolysis by LpL, but not by other lipases (Figure 6E).

Furthermore, heparin affinity profiles showed that the bound fraction, which was seen in group 2 VLDL in the absence of exogenous lipases (marked “native” in Figure 6), was eliminated after hydrolysis by CEase; this hydrolysis also eliminated the IDL/LDL-size particles. In contrast, VLDL treated with other lipases contained both the IDL/LDL-size particles and the bound fraction (Figure 6A, B), while in LpL-treated VLDL, a decrease in the non-bound fraction was accompanied by a decrease in VLDL₁ (Figure 6). These results are consistent with the trend observed in groups 1–3 VLDL showing a direct relation between the population of IDL/LDL-size particles and the bound fraction (Figure 1). This observation further supports the causal link between TG hydrolysis by LpL, which is enhanced upon heparin binding, and the generation of the IDL/LDL-size particles.

Besides lipolysis, other *in vivo* lipoprotein modifications, including proteolysis and oxidation, are enhanced in metabolic disorders such as diabetes ([26] and references therein). We tested how these modifications influence VLDL binding to heparin and subsequent lipoprotein remodeling. Group 2 VLDL were either oxidized by copper or digested by trypsin as described in part 2 Methods, and were analyzed by SEC, heparin affinity chromatography and native PAGE (Figure 6C–E). SEC profiles showed that oxidation and tryptic digestion decreased the population of peak II encompassing VLDL₂/IDL/LDL-size particles as compared to native VLDL (Figure 6C, D compared to A, lower panel). Heparin affinity profiles revealed that upon oxidation, the population of bound

VLDL showed little change but the elution peak shifted to lower salt, from about 0.4 M to 0.25 M NaCl, indicating weaker binding. Moreover, upon tryptic digestion, VLDL binding was largely abolished (Figure 6D), probably because the exposed basic residues in VLDL proteins, which mediate heparin binding, are affected by trypsin either directly (via the proteolytic cleavage at such residues) or indirectly (via the ensuing conformational changes). Importantly, SEC and native PAGE did not detect HDL-size particles in either oxidized or trypsin-treated VLDL (Figure 6C–E).

Collectively, the results in Figure 6 show that hydrolysis of TG in VLDL core by LpL leads to VLDL remodeling into IDL/LDL and HDL-size particles. This remodeling is specific to LpL and is not observed upon any other lipolytic, proteolytic or oxidative modifications. This remodeling closely mimics the metabolic remodeling and maturation of VLDL into IDL/LDL and HDL-like particles *in vivo*, which is driven by LpL and hepatic lipase (reviewed in [1–3]).

3.6 Non-bound VLDL has pro-atherogenic properties

If binding to heparin triggers LpL-induced remodeling of VLDL that mimics its maturation to LDL, then what are the functional properties of the VLDL fraction that does not bind heparin? The major physiological functions of VLDL include delivery of nutrients in the form of LpL-generated NEFA to peripheral cells, and transfer of TG to cholesterol-rich TG-poor lipoproteins, such as HDL and LDL. The latter process is mediated by CETP and involves an equimolar exchange of TG for CE along the gradient; this process contributes to the generation of the pro-atherogenic small dense LDL in hypertriglyceridemia, and CETP inhibition is explored as a therapeutic target for atherosclerosis ([36] and references therein). Here, we explored these functional processes by using bound and non-bound VLDL.

To explore NEFA generation upon TG lipolysis, native and non-bound VLDL were incubated with exogenous LpL (3 h at 37 °C) followed by NEFA quantification. Compared to native VLDL, non-bound VLDL formed poor substrates for the exogenous LpL (Figure S4A). This probably results from higher levels of apoC-III and lower levels of apoC-II in the non-bound fraction (Table 2). For TG transfer, native and non-bound VLDL were incubated with HDL and CETP, VLDL were re-isolated by SEC, and TG were measured as described in part 2 Methods. Non-bound VLDLs formed much more efficient TG donors (Figure S4B), apparently because their initial TG levels were higher while cholesterol ester levels were lower than those in native VLDL (Table 2).

In summary, non-bound VLDLs, which comprise larger TG-rich particles (Figure 2, Table 2), are better TG donors but poorer LpL substrates (Figure S4). Such particles are expected to have increased residence time in plasma, leading to progressive oxidative and hydrolytic modifications, which are pro-atherogenic. Moreover, through the action of LpL and hepatic lipase, large TG-rich VLDL are metabolic precursors of small TG-rich LDL, a particularly pro-atherogenic subclass of plasma lipoproteins [6, 7]. Large TG-rich VLDL can also form precursors of electronegative LDL, a minor LDL subfraction with pro-inflammatory properties [10]. Therefore, non-bound VLDL are expected to have increased pro-atherogenic properties as compared to their bound counterparts. Consequently, heparin affinity chromatography enables us to isolate VLDL subspecies with distinct functionality.

3.7 Changes in heparin binding and VLDL remodeling in diabetes

Next, we tested whether the inverse relationship between VLDL TG levels and binding to heparin, which was observed in healthy subjects (Figure 1, Table 1), extends to diabetic patients. VLDL were isolated from pooled plasma of three groups of donors: normolipidemic controls (NI), patients newly diagnosed with type-2 diabetes prior to treatment (Pc), and the same patients after treatment to improve their glycemic control (Gc); for details see Methods and [26]. Five different VLDL batches were explored. Figure 7 shows representative results of the biochemical analyses along with the heparin affinity and SEC profiles for one batch, and Figure S5 provides similar data for other batches. Compared to NI, Pc VLDL had slightly increased levels of TG, greatly increased apoC-III, and decreased apoC-II (Figure 7A, B), suggesting that Pc VLDL provides a relatively poor substrate for LpL. LpL-dependent VLDL lipolysis verified this conjecture (Figure 7D). In Gc VLDL, the TG levels were restored to normal levels, and the levels apoC-II and C-III, along with the LpL activity, were partially restored (Figure 7A, B, C). Therefore, diabetes treatment to improve glycemic control improves VLDL processing by LpL. Furthermore, in Pc VLDL the baseline levels of NEFA and conjugated dienes were increased compared to NI (Figure 7D, E), reflecting increased lipolysis and oxidation in diabetes. These levels were largely normalized upon treatment, as seen in Gc VLDL.

All SEC and heparin affinity profiles showed similar trends despite batch-to-batch variations (Figure 7 F, G and Figure S5 F, G). Compared to NI controls, Pc VLDL showed a large decrease in the population of both the IDL/LDL-size particles and the bound fraction; moreover, the bound fraction eluted in lower salt, indicating weaker binding to heparin. These effects were partially restored in Gc VLDL, indicating that treatment to improve glycemic control restored, in part, the heparin binding affinity of VLDL as well as its remodeling by the endogenous LpL (Figure 7B). Apolipoprotein glycation, which interferes with heparin binding, must contribute to these effects. In fact, apolipoprotein glycation is increased in diabetes but is largely restored upon treatment to improve glycemic control ([26] and references therein).

In summary, the results of our biochemical, SEC and heparin affinity studies of VLDL from diabetic patients (Figure 7) are consistent with those of normolipidemic VLDL from groups 1–3 (Figure 1). Collectively, these results clearly show that the populations of the IDL/LDL-size particles and the heparin-bound VLDL fraction are directly related to each other and to LpL activity, and increase upon decreasing TG levels in VLDL.

4. DISCUSSION

4.1 Heparin binding activates circulating LpL that remodels VLDL

This study combines heparin affinity chromatography with gel filtration, protein and lipid assays, in vitro lipoprotein remodeling, and other biochemical techniques to examine the causes and effects of VLDL-heparin interactions. The focus is on particle remodeling by LpL in healthy, hypertriglyceridemic and diabetic states. We used pre-heparin plasma, which does not release LpL bound to the endothelium and yields a small amount of circulating LpL associated with lipoproteins. ELISA detected such circulating LpL in normolipidemic

VLDL, and LpL quantities increased in hypertriglyceridemic VLDL (Table 1, groups 1–3). Essentially all LpL was found in VLDL fraction that bound heparin (Figure 4D); this fraction was also enriched in apoE (a major heparin-binding protein) and apoC-II (an activator of LpL), and was depleted of TG (Table 2). Importantly, bound fraction comprised a heterogeneous population of VLDL and remnant particles that underwent rapid remodeling, while the non-bound VLDL was more homogeneous and inert (Figures 2–4). Collectively, the results of this and previous studies [34, 35] show that heparin affinity chromatography enables the isolation of biochemically and metabolically distinct VLDL subclasses.

Although it is well established that a small amount of LpL is bound to circulating VLDL in pre-heparin plasma, physiological role of this LpL was unclear, in part, because of the difficulties in measuring LpL activity in vivo and in retaining LpL distribution and activity in vitro ([2, 3, 19] and references therein). Some studies reported that circulating LpL is catalytically inactive and acts mainly as a bridging molecule [18, 21]. Others observed substantial lipolytic activity of VLDL-associated LpL and proposed it as a relevant metabolic marker, since this activity correlates strongly with plasma VLDL remodeling in healthy state and in diabetes where both VLDL remodeling and the circulating LpL activity are diminished [19, 20].

Our results help reconcile these apparently disparate findings. We show that, although LpL on VLDL isolated from plasma lacks catalytic activity, this LpL is activated upon binding to heparin, triggering rapid TG hydrolysis (Figure 4A). Upon hydrolysis, the particle core shrinks and VLDL is gradually remodeled into smaller IDL/LDL and HDL-size particles along with lipid-poor apolipoproteins (bound VLDL, Figures 2 and 3). These morphologic changes closely resemble the process of VLDL-to-LDL maturation [4]. To our knowledge, such a VLDL remodeling by circulating LpL has not been previously reported, potentially providing an alternative pathway for VLDL maturation in the bloodstream and explaining why the activity of circulating LpL correlates directly and strongly with VLDL remodeling in blood [19, 20].

Although the presence of HS-like molecules bound to circulating VLDL cannot be excluded, detailed mass spectrometry analyses of VLDL have not reported such molecules [37] and, to our knowledge, there is no direct evidence for it. In the absence of such molecules, VLDL remodeling in blood by circulating LpL must occur following VLDL interactions with cell surface proteoglycans.

Notably, even brief binding to heparin (circa 10 min on the heparin-sepharose column) activates LpL, triggering VLDL remodeling (Figure 3). Since the remodeling is inhibited by paraoxon added after heparin affinity chromatography (Figure 4), VLDL-bound LpL must remain catalytically active after dissociating from heparin. We conclude that binding to heparin induces irreversible changes in VLDL-bound LpL stabilizing its active conformation. Molecular details of these changes and the roles of other proteins such as apoCs remain to be determined. One potential mechanism might include stabilization of the active LpL conformation upon heparin binding at a basic molecular face spanning the two lipase domains [15, 16].

4.2 Relevance of VLDL remodeling by circulating LpL to healthy and disease states

VLDL remodeling by the heparin-activated endogenous LpL under near-physiologic solvent conditions *in vitro* occurs over several hours at 22 °C (3–18 h, Figure 3C) and is likely accelerated at 37 °C when LpL activity is increased (Figure 3B). This timeframe is comparable to the residence time of VLDL in plasma (~4 h at 37 °C [6]), suggesting that the remodeling is physiologically relevant.

Analysis of hypertriglyceridemic VLDL (group 3 and a part of group 2) supports this idea. In these TG-rich VLDLs, the LpL levels increase but its catalytic activity decreases, in part, because of the lower apoC-II and higher apoC-III levels (Table 1). As a result of decreased LpL activity, VLDL remodeling and maturation is impaired (Figure 1A, group 3), leading to a classical inverse relation between LpL activity and plasma TG levels [19]. Moreover, binding of TG-rich VLDL to heparin is diminished greatly (Figure 1E), further decreasing VLDL remodeling by LpL; lower levels of the major heparin-binding protein, apoE, probably contribute to this effect (Table 1, group 3). Therefore, despite their decreased structural stability [32], TG-rich VLDLs are expected to have longer residence time in plasma, during which they act as TG donors to LDL and HDL via CETP (Figure S4B) and are progressively oxidized and hydrolyzed. Oxidation and hydrolysis further decrease VLDL affinity for heparin and VLDL remodeling by LpL (Figure 6), perpetuating the vicious cycle. Ultimately, these TG-rich VLDLs give rise to TG-rich LDLs, such as small dense apoC-III-rich LDL [38], which are particularly pro-atherogenic [6–8]. TG-rich VLDL could also form precursors of electronegative LDL, a minor LDL subfraction that is highly pro-inflammatory and pro-atherogenic [10]. Therefore, the results of the current study point to impaired LpL activity as a potential factor contributing to formation of electronegative LDL. Collectively, the results suggest that VLDLs lacking in heparin/HS binding affinity comprise a pro-atherogenic fraction.

Analysis of VLDL from diabetic patients strongly supports this idea. Normolipidemic controls (NI) feature a substantial heparin-bound VLDL fraction, whereas in patients with poor glycemic control (Pc) the bound fraction is nearly abolished, and is partially restored upon treatment that improves glycemic control (Gc) (Figures 7, S5). We propose that in type-2 diabetes, diminished heparin binding impairs VLDL remodeling by circulating LpL, leading to increased population of TG-rich VLDL. Such a diminished heparin binding may result from increased hydrolysis, oxidation (Figure 6) and glycation of diabetic VLDLs. In fact, glycation impairs VLDL turnover [39], and apoE glycation impairs its binding to heparin/HS. The latter may reflect the location of the major glycation site at Lys75 [40] adjacent to the heparin binding site in helix-4 in the 3D structure of apoE [23]; hence, the glycan could potentially interfere with heparin binding at this site in apoE. Collectively, the results suggest heparin affinity chromatography of VLDL as a diagnostic tool and a readout for treatment of metabolic disorders such as hypertriglyceridemia and type-2 diabetes.

4.3 Heparin binding to VLDL versus LDL

Binding to heparin induces irreversible biochemical changes in both LDL and VLDL, yet the molecular basis for these changes and their functional implications are remarkably different. LDL binding to heparin, which is mediated mainly by apoB, induces irreversible

conformational changes in apoB, destabilizes the particle, and augments its hydrolysis, oxidation and fusion ([26] and references therein). These biochemical and structural changes are expected to be strongly pro-atherogenic, which is consistent with clinical studies suggesting proteoglycan binding as a metrics for the pro-atherogenic action of LDL [41].

Unlike LDL, VLDL binding to heparin is mediated mainly by apoE and LpL. The binding activates LpL and accelerates VLDL remodeling into smaller particles (Figures 2–4) culminating in maturation to LDL; this process is non-atherogenic. Additionally, binding to cellular HSPG co-localizes VLDL with its cell receptors and augments its endocytosis, which may be either beneficial (e.g. for normal VLDL uptake via the LDL receptor-related protein in the vascular endothelium) or pathogenic (for VLDL uptake via scavenger receptors on arterial macrophages or cancer cells) [30, 31]. Moreover, our previous study of LDL from NI, Gc, and Pc patients showed that in type-2 diabetes, the heparin-induced pro-atherogenic LDL changes increase [26], while the current study shows that heparin binding to VLDL and the ensuing VLDL remodeling by circulating LpL decrease (Figures 7, S5). Both these phenomena can potentially contribute to the causative link between diabetes and atherosclerosis.

In addition to biochemical differences, differences in the particle size between LDL (20–24 nm) and VLDL (40–100 nm) must also contribute to the distinct effects of HSPG binding by these lipoproteins. LDL is small enough to cross the endothelium, and LDL binding to PGs in the arterial intima favors subendothelial retention and promotes arteriosclerosis [24, 25]. In contrast, VLDLs, most of which are too large to cross the endothelium [25], bind to PGs in the endothelial lumen or on the surface of circulating cells, which promotes VLDL catabolism and is not atherogenic.

4.4 Conclusions

The current study reveals that VLDL-bound LpL can be activated by heparin, which is used as a surrogate for arterial HSPG. This activation triggers VLDL remodeling, which mimics VLDL to LDL maturation and occurs on a timescale of hours, comparable to the residence time of VLDL in plasma. We posit that this remodeling by circulating LpL may represent an additional pathway for VLDL maturation in the bloodstream. Additionally, our results show that heparin-sepharose affinity chromatography provides a one-step tool to isolate and characterize VLDL fractions with distinct biochemical composition and functionality, bound (non-atherogenic) and non-bound (pro-atherogenic). This tool is particularly useful for the identification of VLDL associated with metabolic disorders such as hypertriglyceridemia and type-2 diabetes, as it may help the diagnostics and provide the treatment readout for these major disorders.

Supplementary Material

Refer to Web version on PubMed Central for supplementary material.

Acknowledgements

We are very grateful to Dr. Olivia R. Chavez for recording transmission electron micrographs. We thank Emily Lewkowicz for reading the manuscript prior to publication. This work was funded by the National Institutes of

Health grants RO1 GM026267 and R01 GM135158, and by ISCHII/FIS PI16-00471 from the Spanish Ministry of Health with FEDER funds.

Abbreviations

VLDL	very low-density lipoprotein
IDL	intermediate-density lipoprotein
LDL	low-density lipoprotein
HDL	high-density lipoprotein
apo	apolipoprotein
TG	triacylglycerol
NEFA	non-esterified (free) fatty acids
LpL	lipoprotein lipase
PLA₂	phospholipase A ₂
SMase	sphingomyelinase
CEase	cholesterol esterase
CETP	cholesterol ester transfer protein
HS	heparan sulfate
PG	proteoglycan
NI	normolipidemic
Pc	poor glycemic control
Gc	good glycemic control
SEC	size-exclusion chromatography

References cited

1. Goldberg IJ, 2017 George Lyman Duff Memorial Lecture: Fat in the blood, fat in the artery, fat in the heart: Triglyceride in physiology and disease. *Arterioscler. Thromb. Vasc. Biol* 38(4) (2018) 700–706. [PubMed: 29419410]
2. Wang H, Eckel RH, Lipoprotein lipase: from gene to obesity. *Am. J. Physiol. Endocrinol. Metab* 297(2) (2009) E271–E288. [PubMed: 19318514]
3. Olivecrona G, Role of lipoprotein lipase in lipid metabolism. *Curr. Opin. Lipidol* 27(3) (2016) 233–241. [PubMed: 27031275]
4. Musliner TA, Long MD, Forte TM, Nichols AV, Gong EL, Blanche PJ, Krauss RM, Dissociation of high density lipoprotein precursors from apolipoprotein B-containing lipoproteins in the presence of unesterified fatty acids and a source of apolipoprotein A-I. *J. Lipid Res* 32(6) (1991) 917–933. [PubMed: 1940624]

5. Guha M, England C, Herscovitz H, Gursky O. Thermal transitions in human very-low-density lipoprotein: fusion, rupture, and dissociation of HDL-like particles. *Biochemistry*. (2007) 46(20):6043–6039. [PubMed: 17469851]
6. Demant T, Packard C, In vivo studies of VLDL metabolism and LDL heterogeneity. *Eur. Heart J* 19 Suppl H (1998) H7–H10. [PubMed: 9717058]
7. Berneis KK, Krauss RM, Metabolic origins and clinical significance of LDL heterogeneity. *J. Lipid Res* 43(9) (2002) 1363–1379. [PubMed: 12235168]
8. Vergès B, Abnormal hepatic apolipoprotein B metabolism in type 2 diabetes. *Atherosclerosis*. 211(2) (2010) 353–360. [PubMed: 20189175]
9. Miller M, Stone NJ, Ballantyne C, Bittner V, Criqui MH, Ginsberg HN, Goldberg AC, Howard WJ, Jacobson MS, Kris-Etherton PM, Lennie TA, Levi M, Mazzone T, Pennathur S, Triglycerides and cardiovascular disease: a scientific statement from the American Heart Association. *Circulation*. 123 (2011) 2292–2333. [PubMed: 21502576]
10. Sánchez-Quesada JL, Benítez S, Ordóñez-Llanos J, Electronegative low-density lipoprotein. *Curr. Opin. Lipidol* 15(3) (2004) 3293–3335.
11. Toth PP, Triglyceride-rich lipoproteins as a causal factor for cardiovascular disease. *Vasc. Health Risk Manag* 12 (2016) 171–183. [PubMed: 27226718]
12. Dallinga-Thie GM, Kroon J, Borén J, Chapman MJ, Triglyceride-rich lipoproteins and remnants: targets for therapy? *Curr. Cardiol. Rep* 18(7) (2016) 67. [PubMed: 27216847]
13. Basu D, Goldberg IJ, Regulation of lipoprotein lipase-mediated lipolysis of triglycerides. *Curr. Opin. Lipidol* 31(3) (2020) 154–160. [PubMed: 32332431]
14. Wu SA, Kersten S, Qi L, Lipoprotein lipase and its regulators: An unfolding story. *Trends Endocrinol. Metab* 32(1) (2021) 48–61. [PubMed: 33277156]
15. Birrane G, Beigneux AP, Dwyer B, Strack-Logue B, Kristensen KK, Francone OL, Fong LG, Mertens HDT, Pan CQ, Ploug M, Young SG, Meiyappan M, Structure of the lipoprotein lipase-GPIHBP1 complex that mediates plasma triglyceride hydrolysis. *Proc. Natl. Acad. Sci. USA* 116 (2019) 1723–1732. [PubMed: 30559189]
16. Arora R, Nimonkar AV, Baird D, Wang C, Chiu CH, Horton PA, Hanrahan S, Cubbon R, Weldon S, Tschantz WR, Mueller S, Brunner R, Lehr P, Meier P, Ottl J, Voznesensky A, Pandey P, Smith TM, Stojanovic A, Flyer A, Benson TE, Romanowski MJ, Trauger JW, Structure of lipoprotein lipase in complex with GPIHBP1. *Proc. Natl. Acad. Sci. USA* 116 (2019) 10360–10365. [PubMed: 31072929]
17. Kristensen KK, Leth-Espensen KZ, Mertens HDT, Birrane G, Meiyappan M, Olivecrona G, Jørgensen TJD, Young SG, Ploug M, Unfolding of monomeric lipoprotein lipase by ANGPTL4: Insight into the regulation of plasma triglyceride metabolism. *Proc. Natl. Acad. Sci. USA* 117(8) (2020) 4337–4346. [PubMed: 32034094]
18. Merkel M, Kako Y, Radner H, Cho IS, Ramasamy R, Brunzell JD, Goldberg IJ, Breslow JL, Catalytically inactive lipoprotein lipase expression in muscle of transgenic mice increases very low density lipoprotein uptake: direct evidence that lipoprotein lipase bridging occurs in vivo. *Proc. Natl. Acad. Sci. USA* 95(23) (1998) 13841–13846. [PubMed: 9811888]
19. Pruneta V, Autran D, Ponsin G, Marcas C, Duvillard L, Verges B, Berthezene F, Moulin P, Ex vivo measurement of lipoprotein lipase-dependent very low density lipoprotein (VLDL)-triglyceride hydrolysis in human VLDL: an alternative to the postheparin assay of lipoprotein lipase activity? *J. Clin. Endocrinol. Metab* 86(2) (2001) 797–803. [PubMed: 11158049]
20. Shirakawa T, Nakajima K, Yatsuzuka S, Shimomura Y, Kobayashi J, Machida T, Sumino H, Murakami M, The role of circulating lipoprotein lipase and adiponectin on the particle size of remnant lipoproteins in patients with diabetes mellitus and metabolic syndrome. *Clin. Chim. Acta* 440 (2015) 123–132. [PubMed: 25445417]
21. Sato K, Okajima F, Miyashita K, Imamura S, Kobayashi J, Stanhope KL, Havel PJ, Machida T, Sumino H, Murakami M, Schaefer E, Nakajima T K, The majority of lipoprotein lipase in plasma is bound to remnant lipoproteins: A new definition of remnant lipoproteins. *Clin. Chim. Acta* 461 (2016) 114–125. [PubMed: 27342999]

22. Pruneta V, Pulcini T, Lalanne F, Marçais C, Berthezène F, Ponsin G, Moulin P, VLDL-bound lipoprotein lipase facilitates the cholesteryl ester transfer protein-mediated transfer of cholesteryl esters from HDL to VLDL. *J. Lipid Res* 40(12) (1999) 2333–2339. [PubMed: 10588959]
23. Weisgraber KH, Rall SC Jr., Human apolipoprotein B-100 heparin-binding sites. *J. Biol. Chem* 262(23) (1987) 11097–11103. [PubMed: 3301850]
24. Camejo G, Hurt-Camejo E, Wiklund O, Bondjers G, Association of apo B lipoproteins with arterial proteoglycans: pathological significance and molecular basis. *Atherosclerosis*. 139 (1998) 205–222. [PubMed: 9712326]
25. Borén J, Williams KJ, The central role of arterial retention of cholesterol-rich apolipoprotein-B-containing lipoproteins in the pathogenesis of atherosclerosis: a triumph of simplicity. *Curr. Opin. Lipidol* 27(5) (2016) 473–483. [PubMed: 27472409]
26. Jayaraman S, Chavez OR, Pérez A, Miñambres I, Sánchez-Quesada JL, Gursky O, Binding to heparin triggers deleterious structural and biochemical changes in human low-density lipoprotein, which are amplified in hyperglycemia. *Biochim. Biophys. Acta Mol. Cell Biol. Lipids* 1865(8) (2020) 158712. [PubMed: 32289504]
27. Weisgraber KH, Rall SC Jr., Mahley RW, Milne RW, Marcel YL, Sparrow JT, Human apolipoprotein E. Determination of the heparin binding sites of apolipoprotein E3. *J. Biol. Chem* 261(5) (1986) 2068–2076. [PubMed: 2418019]
28. Pillarisetti S, Paka L, Sasaki A, Vanni-Reyes T, Yin B, Parthasarathy N, Wagner WD, Goldberg IJ, Endothelial cell heparanase modulation of lipoprotein lipase activity. Evidence that heparan sulfate oligosaccharide is an extracellular chaperone. *J. Biol. Chem* 272(25) (1997) 15753–15759. [PubMed: 9188470]
29. Mullick AE, Deckelbaum RJ, Goldberg IJ, Al-Haideri M, Rutledge JC, Apolipoprotein E and lipoprotein lipase increase triglyceride-rich particle binding but decrease particle penetration in arterial wall. *Arterioscler. Thromb. Vasc. Biol* 22(12) (2002) 2080–2085. [PubMed: 12482838]
30. Kobayashi J, Mabuchi H, Lipoprotein lipase and atherosclerosis. *Ann. Clin. Biochem* 52(Pt 6) (2015) 632–637. [PubMed: 25995285]
31. Lupien LE, Bloch K, Dehairs J, Traphagen NA, Feng WW, Davis WL, Dennis T, Swinnen JV, Wells WA, Smits NC, Kuemmerle NB, Miller TW, Kinlaw WB, Endocytosis of very low-density lipoproteins: an unexpected mechanism for lipid acquisition by breast cancer cells. *J. Lipid Res* 61(2) (2020) 205–218. [PubMed: 31806729]
32. Jayaraman S, Baveghems C, Chavez OR, Rivas-Urbina A, Sánchez-Quesada JL, Gursky O, Effects of triacylglycerol on the structural remodeling of human plasma very low- and low-density lipoproteins. *Biochim. Biophys. Acta Mol. Cell. Biol Lipids* 1864(7) (2019) 1061–1071. [PubMed: 30844432]
33. Sacks FM, The crucial roles of apolipoproteins E and C-III in apoB lipoprotein metabolism in normolipidemia and hypertriglyceridemia. *Curr. Opin. Lipidol* 26(1) (2015) 56–63. [PubMed: 25551803]
34. Huff MW, Telford DE, Characterization and metabolic fate of two very-low-density lipoprotein subfractions separated by heparin-sepharose chromatography. *Biochim. Biophys. Acta* 796(3) (1984) 251–261. [PubMed: 6509076]
35. Duvillard L, Caslake MJ, Petit JM, Vergès B, Gambert P, Packard CJ, Distinct patterns of heparin affinity chromatography VLDL1 and VLDL2 subfractions in the different dyslipidaemias. *Atherosclerosis*. 199(1) (2008) 27–33. [PubMed: 18177876]
36. Kettunen J, Holmes MV, Allara E, Anufrieva O, Ohukainen P, Oliver-Williams C, Wang Q, Tillin T, Hughes AD, Kähönen M, Lehtimäki T, Viikari J, Raitakari OT, Salomaa V, Järvelin MR, Perola M, Davey Smith G, Chaturvedi N, Danesh J, Di Angelantonio E, Butterworth AS, Ala-Korpela M, Lipoprotein signatures of cholesteryl ester transfer protein and HMG-CoA reductase inhibition. *PLoS Biol.* 17(12) (2019) e3000572. [PubMed: 31860674]
37. Dashty M, Motazacker MM, Levels J, de Vries M, Mahmoudi M, Peppelenbosch MP, Rezaee F, Proteome of human plasma very low-density lipoprotein and low-density lipoprotein exhibits a link with coagulation and lipid metabolism. *Thromb. Haemost* (2014) 111(3):518–530. [PubMed: 24500811]

38. Gaubatz JW, Gillard BK, Massey JB, Hoogveen RC, Huang M, Lloyd EE, Raya JL, Yang CY, Pownall HJ, Dynamics of dense electronegative low density lipoproteins and their preferential association with lipoprotein phospholipase A(2). *J Lipid Res.* (2007) 48(2):348–357. [PubMed: 17102149]
39. Mamo JC, Szeto L, Steiner G, Glycation of very low density lipoprotein from rat plasma impairs its catabolism. *Diabetologia.* 33(6) (1990) 339–345. [PubMed: 2379765]
40. Laffont I, Shuvaev VV, Briand O, Lestavel S, Barbier A, Taniguchi N, Fruchart JC, Clavey V, Siest G, Early-glycation of apolipoprotein E: effect on its binding to LDL receptor, scavenger receptor A and heparan sulfates. *Biochim. Biophys. Acta* 1583(1) (2002) 99–107. [PubMed: 12069854]
41. Steffen HLM, Anderson JLC, Poot ML, Lei Y, Connelly MA, Bakker SJL, Öörni K, Tietge UJF, Proteoglycan-binding as pro-atherogenic function metric of apoB-containing lipoproteins and chronic kidney graft failure. *J. Lipid Res* 62 (2021) 100083. [PubMed: 33939983]

Highlights:

- Lipoprotein lipase (LpL) that circulates on VLDL is catalytically inactive
- We report that transient binding to heparin activates this VLDL-bound LpL
- VLDL remodeling upon such activation resembles VLDL-to-LDL maturation
- Impaired VLDL remodeling in diabetes is associated with atherosclerosis
Heparin binding affinity provides a readout for VLDL functionality

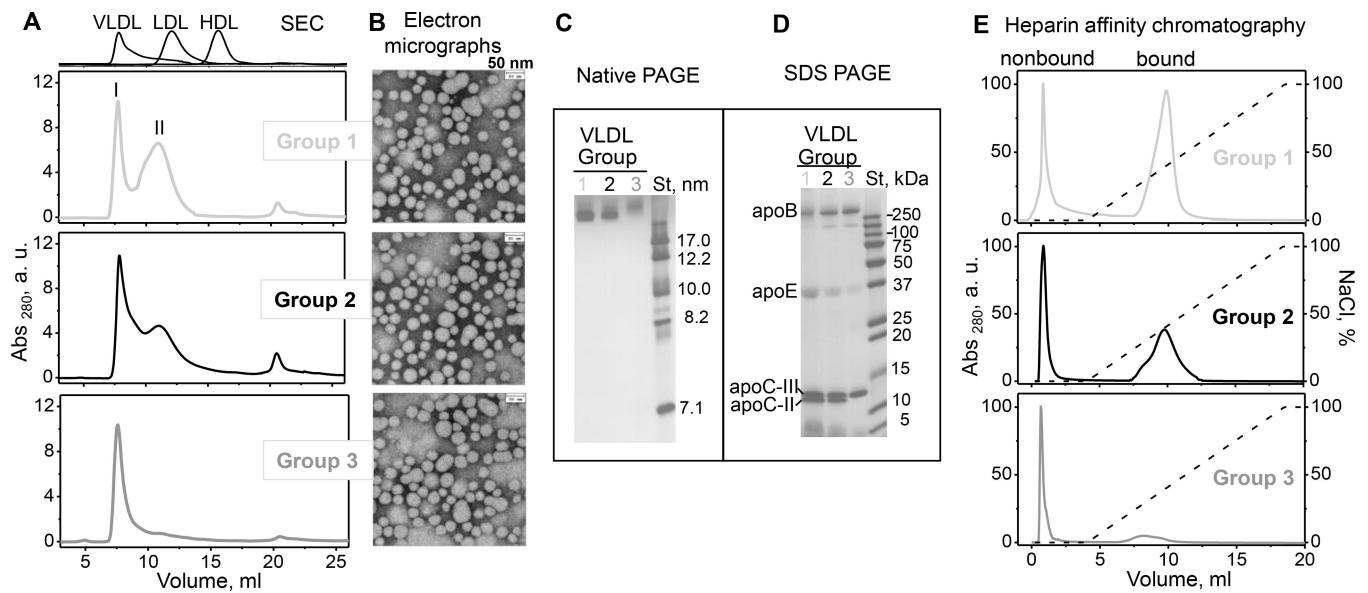


Figure 1.

Characterization of single-donor VLDL isolated from plasma of three representative healthy donors from groups 1 (light grey), 2 (black) and 3 (dark grey) (low, medium and high TG). Table 1 shows biochemical composition of these VLDL.

(A) SEC profiles and (B) transmission electron micrographs of VLDL groups 1 to 3 (top to bottom). Peaks I and II, which correspond to VLDL subclasses VLDL₁ (large buoyant) and VLDL₂ (small dense), are indicated (see supplemental Figure S4 for details). Elution profiles of freshly isolated single-donor human HDL, LDL and VLDL are shown for reference (top).

(C) Non-denaturing PAGE and (D) SDS PAGE of VLDL groups 1 to 3 (left to right). St – molecular standards. Bands corresponding to the major VLDL apolipoproteins are labeled in panel D.

(E) Heparin-sepharose chromatography profiles of VLDL. Bound and non-bound fractions are labeled. The dotted line indicates the calculated NaCl concentration (100% corresponds to 1.01 M NaCl).

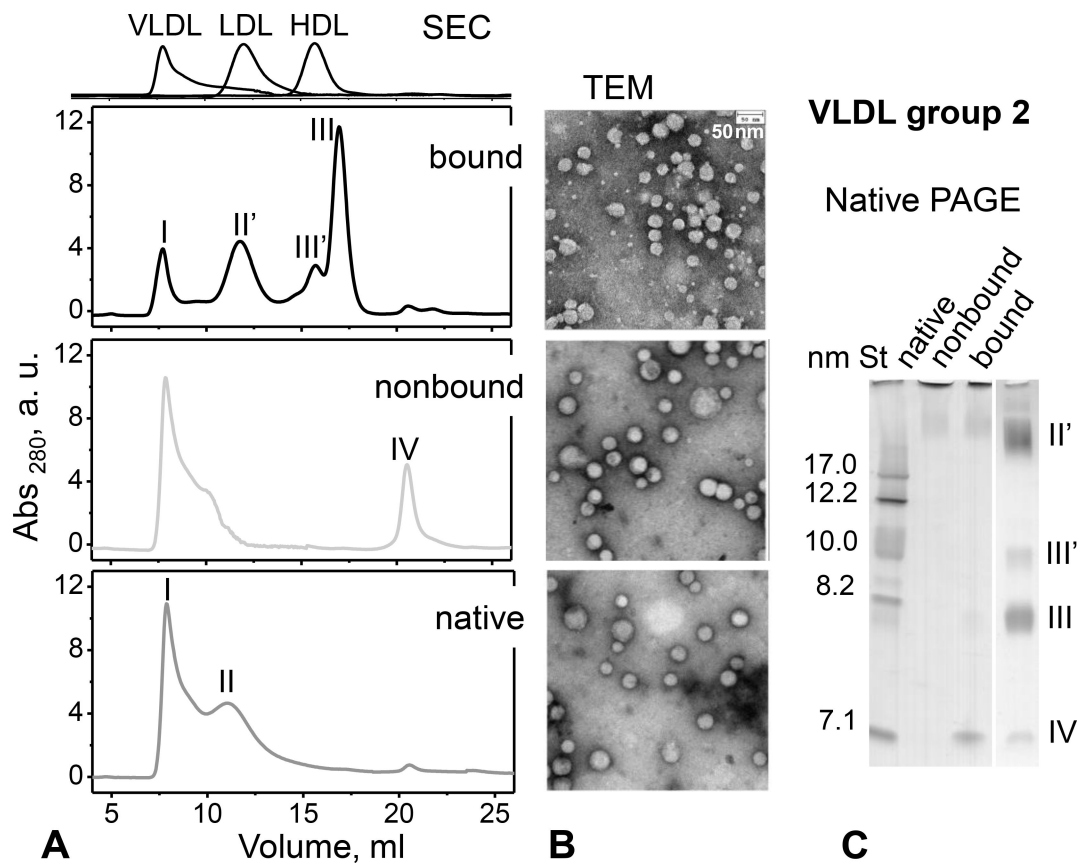


Figure 2.

Particle size distribution in heparin-bound and non-bound fractions of VLDL from group 2. The fractions were separated by heparin affinity chromatography as shown in Figure 1E (middle panel) and used 6 hours thereafter. Native VLDL (before separation) is shown for comparison. Table 2 lists the biochemical composition of these VLDLs measured approximately 6 hours after the separation by heparin affinity. (A) SEC profiles and (B) transmission electron micrographs of bound, non-bound and native VLDL (top to bottom). Elution profiles of freshly isolated single-donor human HDL, LDL and VLDL are shown at the top of panel A for comparison. (C) Non-denaturing PAGE of these VLDLs (8 μ g of total protein per lane). St – molecular size standards. Particles in the size range of intact VLDL (I, circa 40–80 nm), IDL/LDL (II', circa 20–30 nm), HDL (III and III', ~8 nm and ~10 nm) and lipid-poor proteins (IV, ~7 nm) are indicated in panels A and C.

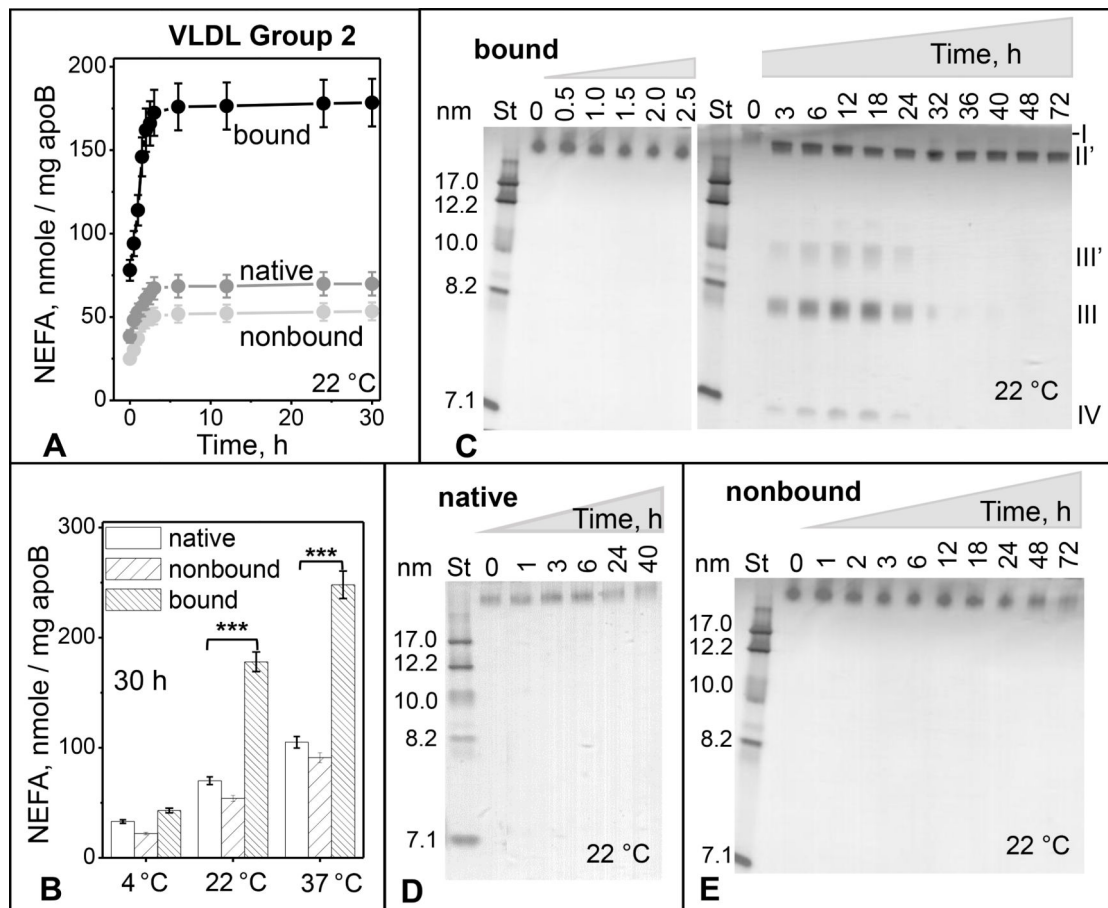


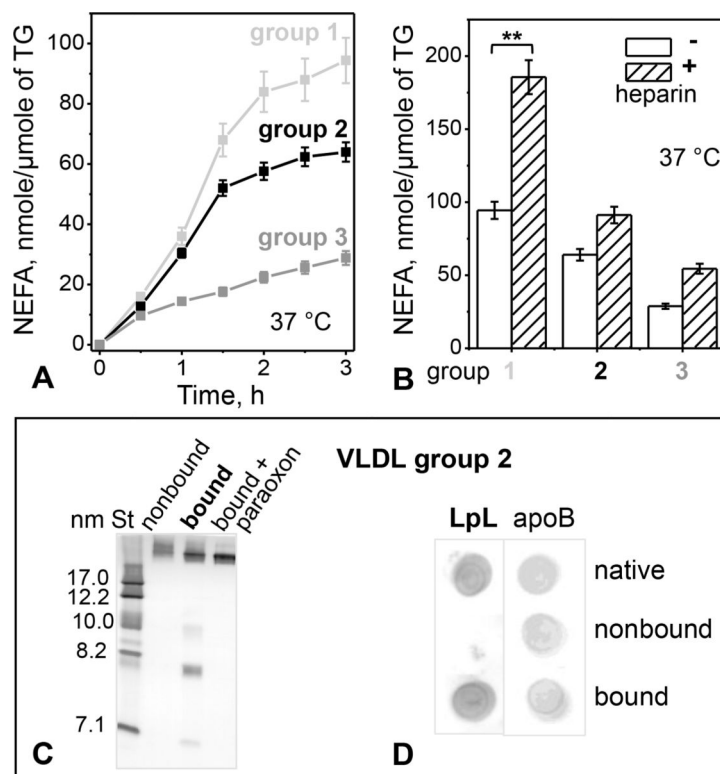
Figure 3.

Time and temperature dependence of spontaneous lipolysis and remodeling of group 2 VLDL.

(A) Time course of total lipolysis. Immediately after separation by heparin affinity chromatography, bound and non-bound VLDL fractions along with native VLDL (0.5 mg/ml total protein) were incubated in buffer A at 22 °C for up to 30 h (see part 2 Methods for details). NEFA levels were measured at indicated time points. The results are shown as the mean \pm SEM of three independent measurements.

(B) Temperature dependence of total lipolysis. VLDL (0.5 mg/ml protein) in buffer A was incubated for 30 h at 4 °C, 22°C or 37 °C, whereupon NEFA were quantified as described in part 2 Methods. Statistically significant differences between bound and native VLDL are indicated (***, $p < 0.05$).

(C-E) Time course of particle remodeling at 22 °C for bound (C), native (D), and non-bound VLDL (E). VLDL (0.5 mg/ml protein) in buffer A was incubated for 42–72 h, sample aliquots were taken at indicated time points, cooled on ice, and immediately analyzed by non-denaturing PAGE. St – molecular size standards. Band positions corresponding to the size of intact VLDL (I), IDL/LDL (II'), HDL (III' and III), and lipid-poor protein (IV) are indicated in panel C.

**Figure 4.**

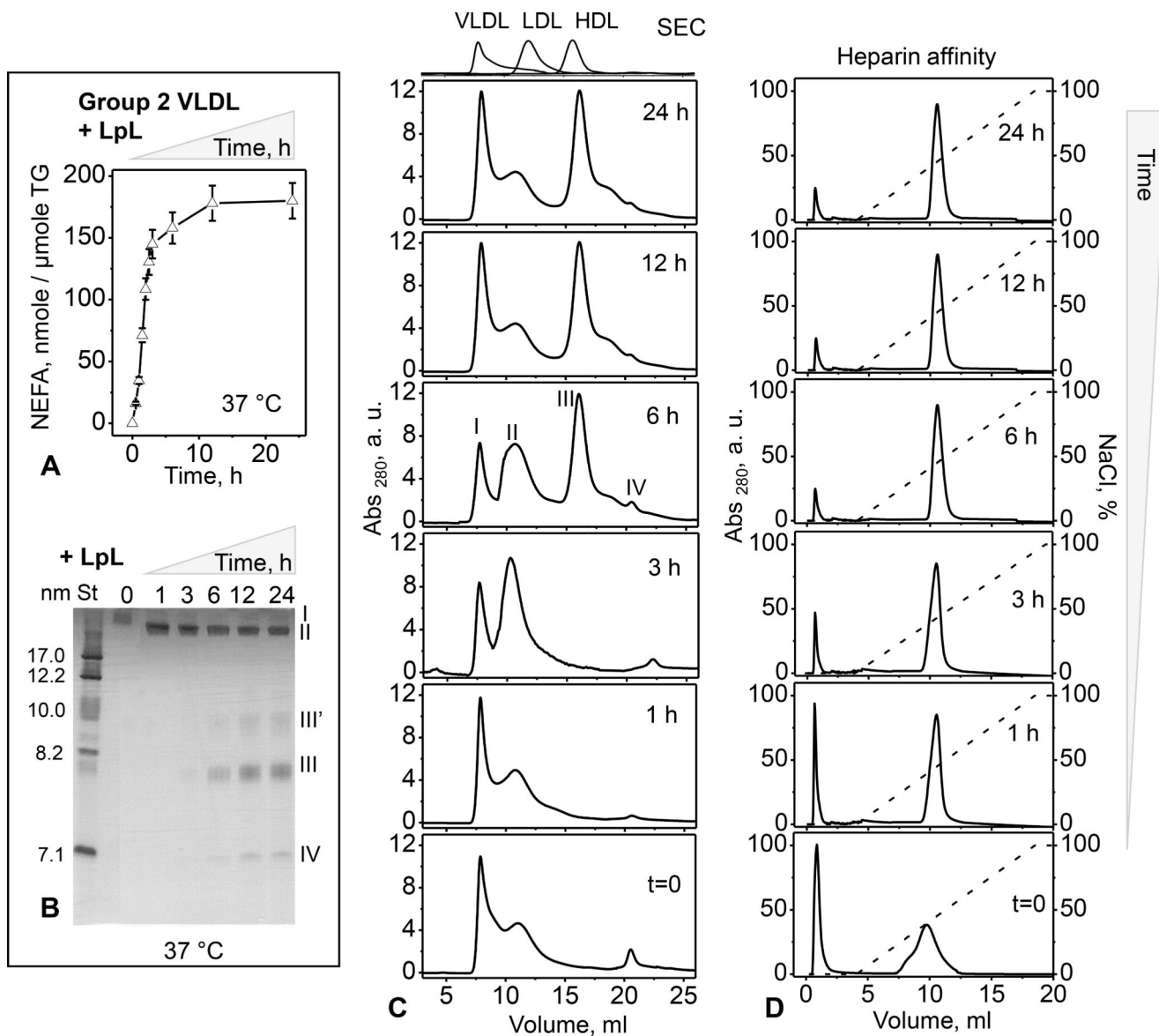
LpL-dependent hydrolysis of TG in VLDL.

(A) Time course of lipolysis by the endogenous VLDL-bound LpL. VLDLs (0.3 μ mole TG) from groups 1 – 3 were incubated without or with paraoxon (2 mmol/ml) at 37 °C for to 3 h. NEFA were measured at indicated time points; the blanks (with LpL inhibited by paraoxon) were subtracted from the data (without paraoxon). The results are shown as the mean \pm SEM of three independent measurements.

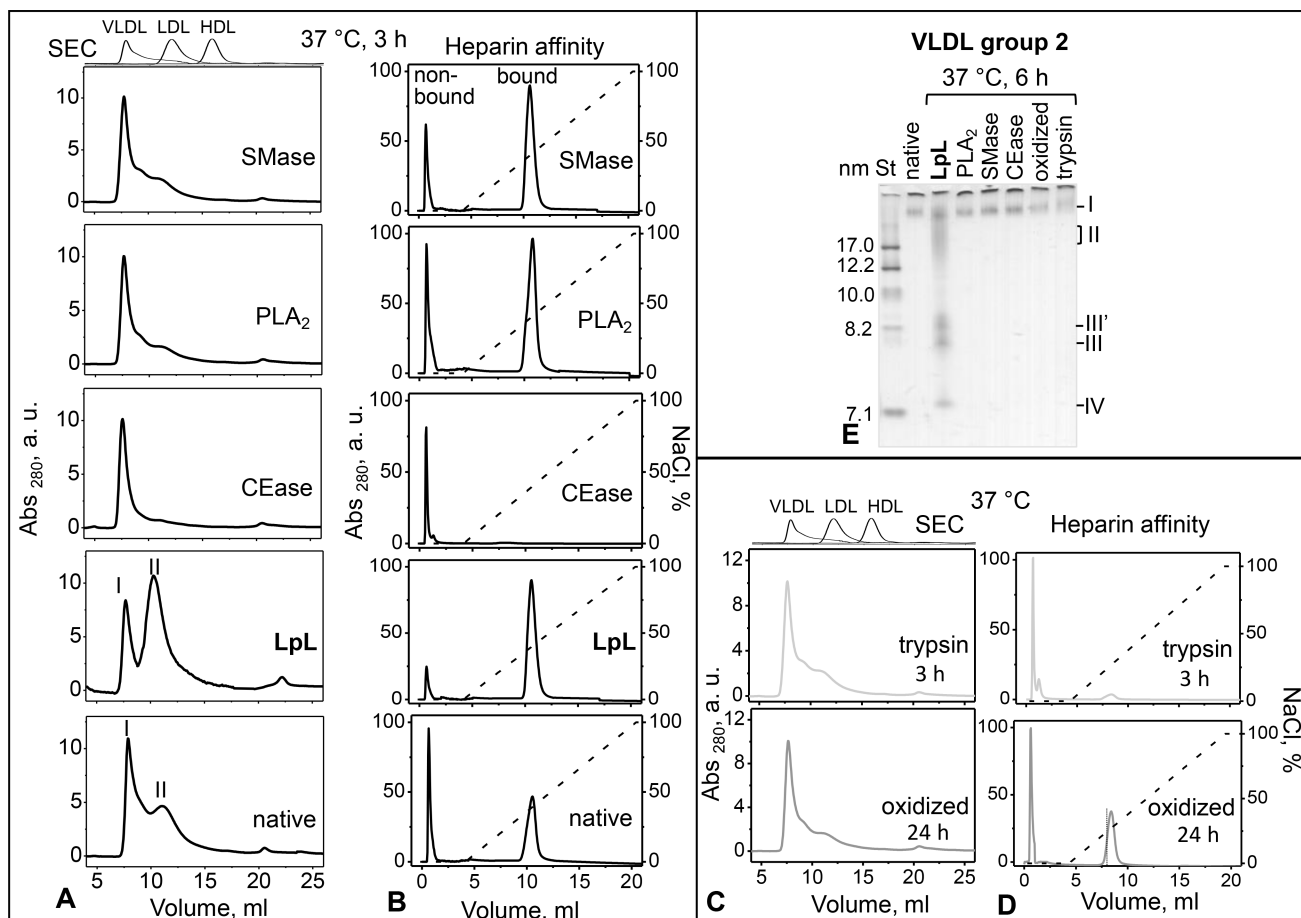
(B) Heparin augments TG hydrolysis by the endogenous VLDL-bound LpL. VLDL (0.3 μ mole TG) was incubated with heparin (0.3 μ g/ml) at 37 °C for 3 h, the reaction was stopped with paraoxon (2 mmol/ml), whereupon NEFA were quantified. Values are shown as the mean \pm SEM of three independent measurements; p 0.1 (**), p 0.05 (***)

(C) Non-denaturing PAGE of group 2 VLDL 6 hours after fractionation by heparin affinity chromatography. Non-bound fraction, bound fraction without or with paraoxon, and molecular size standards (St) are shown.

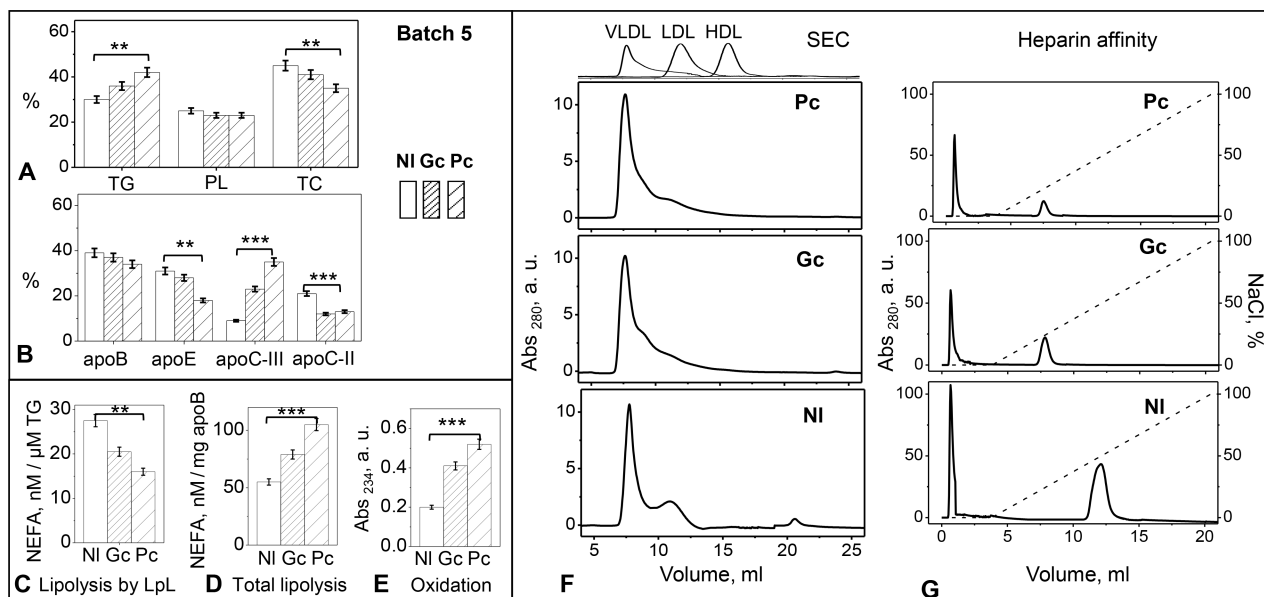
(D) Dot blot of VLDL 6 hours after fractionation by heparin affinity (same as in panel C) using antibodies for LpL and apoB.

**Figure 5.**

VLDL remodeling by the exogenous LpL. (A) Time course of TG lipolysis in group 2 VLDL by bovine LpL (see part 2 Methods for details). The reaction was monitored by quantifying NEFA at indicated time points. (B) Non-denaturing PAGE of VLDL after lipolysis by LpL for indicated times. Band positions corresponding to the particle size of intact VLDL (I), IDL/LDL (II), HDL (III' and III) and lipid-poor proteins (IV) are indicated. (C) SEC and (D) heparin affinity profiles of VLDL hydrolyzed for indicated times. Peaks I-IV are indicated. The dotted line in D represents the calculated NaCl concentration (100% corresponds to 1.01 M NaCl).

**Figure 6.**

Effects of VLDL lipolysis, proteolysis and oxidation on the particle remodeling and heparin binding affinity. (A) SEC and (B) heparin affinity profiles of group 2 VLDL which was either native or has been hydrolyzed by LpL, CEase, PLA₂, or SMase for 3 h at 37 °C as described in part 2 Methods. (D) SEC and (E) heparin affinity profiles of VLDL that has been oxidized by copper for 24 h or proteolyzed by trypsin for 3 h at 37 °C, as described in Methods. Dotted line in the heparin affinity profiles represents the NaCl concentration (100% stands for 1.01 M NaCl). (E) Non-denaturing PAGE of VLDL that were either native or modified for 6 h at 37 °C by LpL, PLA₂, SMase, CEase, oxidation, or trypsin digestion (indicated on the lanes). Bands containing particles in the size range of intact VLDL (I), IDL/LDL (II), HDL (III', III) and lipid-poor protein (IV) are indicated.

**Figure 7.**

Characterization of VLDL from normolipidemic (NI) and type-2 diabetic patients before (Pc) and after treatment (Gc). Data for one representative batch are shown; similar data for other batches are shown in supplemental Figure S5. (A) Lipid and (B) protein analysis of intact VLDL. PL – phospholipids, TC – total cholesterol. (C) Spontaneous TG lipolysis by the endogenous LpL and (D) total lipolysis of VLDL. (E) Oxidation index of freshly isolated VLDL measured by absorbance at 234 nm for conjugated dienes. (F) SEC and (G) heparin affinity profiles of VLDL. Moderate ($p < 0.1$, **) and significant differences ($p < 0.05$, ***) between Pc and NI values are indicated.

Table 1.

Biochemical composition of single-donor plasma VLDL from groups 1 to 3. Representative data for one donor from each group are shown. The trends that are reproducible for all donors within each group are shown by arrows indicating increase (↑) or decrease (↓) from group 1 to group 3. TG - triacylglycerol; PL – phospholipid (total); Ch - cholesteryl (total); FC - unesterified (free) cholesterol; CE – cholesterol ester. The lipids were quantified by enzymatic assays as described in Methods. The proteins were quantified by ELISA. The values are shown as % of total lipid weight or total protein weight, except for NEFA and LpL, which are presented in nM or ng per mg of apoB, respectively. The values represent the mean of three independent experiments ± SEM. Decrease in the surface constituents, apoB and FC, is consistent with decreased average particle size due to decrease in VLDL₂ fraction from group 1 to 3 (Figures 1A and S2). PL, which generally varies the least as weight %, does not show any significant changes; changes in PL could be offset by changes in FC and apolipoproteins.

	Group-1	Group-2	Group-3	
Lipid, %				
TG	32.0 ± 1.5	40.0 ± 1.2	48.0 ± 1.2	↑
PL	25.6 ± 1.9	27.2 ± 1.8	25.7 ± 1.6	—
Ch	18.3 ± 1.1	16.4 ± 1.2	13.1 ± 1.4	↓
FC	9.1 ± 1.3	5.1 ± 1.1	4.1 ± 1.8	↓
CE	15.0 ± 1.8	11.3 ± 1.1	9.1 ± 1.6	↓
NEFA, nM/mg apoB	72 ± 15	65 ± 13	59 ± 16	
Protein				
apoB, %	47 ± 1.9	45 ± 1.3	38 ± 1.7	↓
apoE, %	25 ± 1.4	22 ± 1.4	12 ± 1.1	↓
apoC-III, %	9 ± 1.1	21 ± 1.9	41 ± 1.9	↑
apoC-II, %	19 ± 1.8	12 ± 1.0	9 ± 1.1	↓
LpL, ng/mg apoB	18.6 ± 1.1	21.1 ± 1.7	37.6 ± 1.2	↑

Table 2.

Biochemical composition of nonbound and bound fractions isolated from the same VLDL batch by heparin-sepharose affinity chromatography. Native VLDL (before chromatography) is shown for comparison. Representative data for a single donor from group 2 are shown; the trends are reproducible for all donors within the same group. The corresponding chromatographic profile for group 2 VLDL is shown in Figure 1E (middle panel). TG - triacylglycerol; PL – phospholipid (total); Ch - cholesteryl (total); FC - unesterified (free) cholesterol; CE – cholesterol ester. NEFA values (in nM/mg of apoB), which change over time as shown in Figure 3A below, are provided 6 hours after the isolation of bound VLDL when NEFA values level off. The lipids were quantified by enzymatic assays as described in Methods. The proteins were quantified by ELISA. The values, shown as % of total lipid weight or total protein weight, represent the mean of three independent experiments, with the accuracy of $\pm 2\%$. Although LpL has not been quantified, the dot blot data (Figure 4D) show LpL in bound and in native VLDL but not in the nonbound VLDL (indicated by + or –).

	Native	Nonbound	Bound
Lipid, %			
TG	40.0 \pm 1.2	57.0 \pm 1.6 ***	8.3 \pm 1.2 ***
PL	27.2 \pm 1.8	23.8 \pm 1.9	28.5 \pm 1.4
Ch	16.4 \pm 1.2	10.1 \pm 1.1 ***	33.6 \pm 1.8 ***
FC	5.1 \pm 1.1	3.4 \pm 1.1 **	11.8 \pm 1.9 ***
CE	11.3 \pm 1.4	5.7 \pm 1.4 ***	17.8 \pm 1.9 ***
NEFA, nM/ mg apoB	65 \pm 7.1	52 \pm 17	170 \pm 15 ***
Protein, %			
apoB	45 \pm 1.4	42 \pm 1.1	35 \pm 1.7 **
apoE	22 \pm 1.9	7 \pm 1.5 ***	39 \pm 1.4 ***
apoC-III	21 \pm 1.2	49 \pm 1.5***	11 \pm 1.9 ***
apoC-II	12 \pm 1.4	2 \pm 1.4 ***	15 \pm 1.7
LpL	+	-	+

The results are shown as the mean \pm SEM of three independent measurements; p 0.1 (**), p 0.05